HHS Public Access

Author manuscript

*J Immunol*. Author manuscript; available in PMC 2024 December 10.

Published in final edited form as:

*J Immunol*. 2021 July 01; 207(1): 115–124. doi:10.4049/jimmunol.2100115.

# TLR and IKK complex mediated innate immune signaling inhibits stress granule assembly

**Parimal Samir**[1], **David E. Place**[1], **R. K. Subbarao Malireddi**[1], **Thirumala-Devi Kanneganti**[1,*]

[1]Department of Immunology, St. Jude Children's Research Hospital, Memphis, TN, 38105, USA

## Abstract

Cellular stress can induce cytoplasmic ribonucleoprotein complexes called stress granules that allow the cells to survive. Stress granules are also central to cellular responses to infections, where they can act as platforms for viral replication and modulate innate immune signaling through pattern recognition receptors (PRRs). However, the effect of innate immune signaling on stress granules is poorly understood. Here, we report that prior induction of innate immune signaling through Toll-like receptors (TLRs) inhibited stress granule assembly in a TLR ligand dose-dependent manner in murine bone marrow-derived macrophages (BMDMs). Time course analysis suggests that TLR stimulation can reverse stress granule assembly even after it has begun. Additionally, both MYD88- and TRIF-mediated TLR signaling inhibited stress granule assembly in response to endoplasmic reticulum stress in BMDMs and the chemotherapeutic drug oxaliplatin in murine B16 melanoma cells. This inhibition was not due to a decrease in expression of the critical stress granule proteins G3BP1 and DDX3X and was independent of IRAK1/4, JNK, ERK and P38 kinase activity but dependent on IKK complex kinase activity. Overall, we have identified the TLR-IKK complex signaling axis as a regulator of stress granule assembly-disassembly dynamics, highlighting crosstalk between processes that are critical in health and disease.

### Keywords

DDX3X; G3BP1; TLR2; TLR3; TLR4; TLR7/8; stress granules; MYD88; TRIF; MAP Kinase signaling; ERK1/2; eIF2a; JNK; P38; IKK complex

## INTRODUCTION

Stress granules are cytoplasmic membraneless compartments formed in response to some stressors (1–3). They are thought to store translation initiation machinery to allow cells to survive until the stressor is removed. Additionally, stress granules can modulate the innate immune response. They can prevent excess inflammation by inhibiting NLRP3

[*]**Correspondence to:** Thirumala-Devi Kanneganti, Department of Immunology, St. Jude Children's Research Hospital, MS #351, 262 Danny Thomas Place, Memphis TN 38105-3678, Fax. (901) 595-5766. Thirumala-Devi.Kanneganti@StJude.org.

AUTHOR CONTRIBUTIONS

P.S., and T.-D.K. conceptualized the study; P.S., and T.-D.K. designed the experiments; P.S., R.K.S.M and D.P., performed the experiments; P.S., and T.-D.K. conducted the analyses; P.S. wrote the first draft of the manuscript; all authors reviewed and approved the final manuscript; T.-D.K. supervised the project and provided guidance.

COMPETING FINANCIAL INTERESTS

The authors declare no competing financial interests.

inflammasome-driven pyroptosis in bone marrow-derived macrophages (BMDMs) (4), and they can increase the innate immune response to viral infections (5–11). While the impact of stress granules on the innate immune system is becoming increasingly clear, the inverse relationship, or the effect of innate immune signaling on stress granules, has not been investigated.

Our current understanding of the molecular pathways activated in response to stressors suggests a potential for crosstalk between stress granule assembly and innate immune signaling. For instance, the stress responsive MAP kinases (SAPK's) P38 and JNK are activated in response to stressors that induce stress granules (12). SAPK's are also activated by Toll-like receptor (TLR) signaling (13). TLRs are pattern recognition receptors (PRRs) that sense pathogen- and damage-associated molecular patterns (PAMPs and DAMPs) to help mount innate immune response to pathogenic challenges. Although SAPK's are induced by both stress granule-inducing stressors and TLR stimulation in isolation, it remains unclear how the activation of the innate immune response influences stress granule dynamics and the molecular mechanisms involved in this crosstalk. In this study, we discovered that the inhibitor of nuclear factor-κB (IκB) kinase (IKK) complex inhibits stress granule assembly downstream of TLR signaling.

## METHODS

### Mice

*Myd88*$^{-/-}$ *Trif*$^{-/-}$ mice have been described previously (14). All mice were bred at St. Jude Children's Research Hospital, and animal studies were conducted in accordance with protocols approved by the St. Jude Animal Care and Use Committee.

### Cell culture and stimulations

Primary BMDMs were grown for 6 days in IMDM (Thermo Fisher Scientific, 11995–073) supplemented with 10% FBS (Biowest, S1620), 30% L929-conditioned medium and 1% penicillin and streptomycin (Sigma Aldrich). BMDMs were seeded in 12-well plates at a density of $1 \times 10^6$ cells per well and incubated overnight before stimulation. To induce stress granule formation, BMDMs were washed with PBS, incubated with DMEM supplemented with 10% FBS for 1 hour followed by treatment as indicated in figure legends. Pam3CSK4 (Invivogen, tlrl-pms) at a concentration of 1 μg/mL was used to stimulate TLR2. Low molecular weight poly(I:C) (Invivogen, tlrl-picw-250) at a concentration of 50 μg/mL was used to stimulate TLR3. Ultrapure LPS (E. coli 0111:B4, Invivogen, tlrl-3pelps) at a concentration of 100 ng/mL was used to stimulate TLR4. In the LPS dose response experiment, the concentrations used were 1 ng/mL, 10 ng/mL, 100 ng/mL, and 1000 ng/mL. R848 (Resiquimod) (Invivogen, tlrl-r848–5) at a concentration of 1 μg/mL was used to stimulate TLR7/8. SB203580 (Selleckchem, S1076) and U0126 (Cayman Chemicals, 70970) were used at the concentration of 10 μM to inhibit P38 and ERK1/2, respectively. SP600125 (Selleckchem, S1460) was used at the concentration of 25 μM to inhibit JNK. BMS345541 (Selleckchem, S8044) at the concentration of 20 μM was used to inhibit IKK complex. Thapsigargin (Cayman Chemicals, 10522) was used at a concentration of 2 μg/mL. IRAK1/4 inhibitor (MedChemExpress, HY-13329) was used at a concentration of 5 μM to

inhibit IRAK1 and IRAK4 kinases. B16 melanoma cells were stimulated with 100 ng/mL LPS, 50 μg/mL poly(I:C), or 2 μg/mL R848 for 4 hours followed by 4 hours of 100 μM oxaliplatin treatment (Cayman Chemicals, 13106).

### Immunoblotting analysis

Following stimulations, cells were lysed in RIPA buffer followed by boiling them after adding sample loading buffer containing SDS and 2-mercaptoethanol. Protein samples were separated on 8%, 10%, or 12% polyacrylamide gels and then transferred onto PVDF membranes (Millipore). Membranes were blocked in 5% skim milk and incubated with the desired primary antibodies overnight and subsequently with near infra-red dye (IR-dye) or HRP conjugated secondary antibodies. Primary antibodies used in this study were anti-DDX3X (Bethyl Laboratories, A300–474A, 1:1000), anti-G3BP1 (Proteintech, 27299-I-AP, 1:1000), anti–phospho-eIF2α (CST, 3398, 1:1000), anti-eIF2α (CST, 9722, 1:1000) anti–phospho-ERK1/2 (#9101, CST, 1:1000), anti-ERK1/2 (#9102, CST, 1:1000), anti–phospho-P38 (#9211, CST, 1:1000), anti-P38 (#9212, CST, 1:1000), anti–phospho-JNK (#9251, CST, 1:1000), anti-JNK (#9252, CST, 1:1000), anti–phospho-IκBα (#2859, CST, 1:1000), anti-IκBα (#9242, CST, 1:1000), anti–phospho-RPS6 (#, CST, 1:1000), anti–phospho-AKT (#4691, CST, 1:1000), anti–phospho-IKKβ (#2697, CST, 1:1000), anti-IKKβ (#2370, CST, 1:1000), rhodamine conjugated anti-actin (BioRad Laboratories, 1:10000). IR dye conjugated secondary antibodies Amersham CyDye 700 goat-anti-mouse, (#29360785, GE Life Sciences, 1:5000) or Amersham CyDye 800 goat-anti-rabbit (#29360791, GE Life Sciences, 1:5000), or appropriate HRP-conjugated secondary antibody (Jackson Immuno Research Laboratories anti-rabbit (111–035-047) and anti-mouse (315–035-047)) with Luminata Forte Western HRP Substrate (Millipore, WBLUF0500) were used. The proteins were detected on a BioRad Gel Imager (BioRad Laboratories) or Amersham Imager 600 (GE Life Sciences).

### Confocal microscopy imaging

Following stimulations of BMDMs, cells were fixed in 4% paraformaldehyde (ChemCruz) at room temperature for 15 min and washed with PBS. Blocking was done in 10% normal goat serum (Sigma) in PBS. To stain stress granules, BMDMs were stained with the following antibodies at room temperature for 2 h or overnight at 4°C: anti-G3BP1 (27299-I-AP, Proteintech, 1:250) and anti-DDX3X (A300–474A, Bethyl Laboratories, 1:250). BMDMs were incubated with the following secondary antibodies: Alexa Fluor 488-conjugated anti-mouse IgG (R37120, Life Technologies, 1:250), Alexa Fluor 568-conjugated anti-rabbit IgG (A-11011, Life Technologies, 1:250) and DAPI (2 μg/mL). Confocal images were acquired on either a Leica SP8 (Leica Microsystems) or Marianas (Intelligent Imaging Innovations, Inc) confocal microscope.

### Quantitatve reverse transcription polymerase chain reaction

qRT-PCR analysis was performed as previously described (15) with fhe following primers: *Il1b*-For GACCTTCCAGGATGAGGACA, *Il1b*-Rev AGCTCATATGGGTCCGACAG, *Ifnb*-For CAGCTCCAAGAAAGGACGAAC, *Ifnb*-Rev GGCAGTGTAACTCTTCTGCAT.

### Statistical analysis

Statistical significance of the data was determined by the unpaired two-tailed *t*-test or one-way and two-way ANOVA methods as indicated in the figure legends. Mean and error bars represent standard error of mean (s.e.m.). GraphPad Prism v8 software was used for statistical analysis.

## RESULTS

### TLR4 stimulation inhibits stress granule assembly

To test the effect of innate immune signaling mediated by PRRs on stress granules, we stimulated a well characterized PRR, TLR4, with its ligand lipopolysaccharide (LPS) to activate downstream signaling pathways in bone marrow-derived macrophages (BMDMs). We then used the endoplasmic reticulum stress-inducing agent thapsigargin to induce stress granules (16). No cells formed stress granules in the media alone or LPS-treated populations, suggesting LPS treatment on its own does not induce stress granule assembly (Fig. 1A). Thapsigargin treatment robustly induced stress granules in unprimed BMDMs. However, the percentage of cells with stress granules was significantly reduced in LPS-primed BMDMs (Fig. 1B), suggesting that prior activation of TLR4 signaling is sufficient to inhibit stress granule assembly induced by ER stress. To determine whether the dose of LPS impacted the ability for TLR signaling to inhibit stress granule assembly, we tested a range of concentrations from 1 ng/mL to 1000 ng/mL. Stress granule inhibition was dose-dependent, and fewer stress granules were formed as the concentration of LPS increased, with the two highest concentrations (100 ng/mL and 1000 ng/mL) causing similar stress granule inhibition (Supplemental Fig. 1A, 1B). Therefore, we chose to use 100 ng/mL of LPS for subsequent experiments. Overall, TLR4 stimulation robustly inhibited stress granule assembly induced by thapsigargin treatment.

### Signaling downstream of both MYD88 and TRIF can inhibit stress granule assembly

TLR4 can engage both MYD88 and TRIF adaptors to activate downstream signaling, and TLR4 can be found on both the plasma membrane and endosomes (17, 18). Other TLRs are more selective in their adaptor engagement and localization. TLR7/8 engages MYD88 and is localized to endosomes. TLR2 also engages MYD88 but is localized to plasma membranes. TLR3 engages TRIF and is localized to endosomes. Therefore, testing the effects of signaling through these TLRs on stress granule formation can resolve the roles of MYD88- and TRIF-mediated signal transduction as well as subcellular localization in regulating stress granule assembly. To determine which adaptors are involved in stress granule inhibition, we stimulated TLR2, TLR3, and TLR7/8 with their ligands Pam3CSK4, poly(I:C), and R848, respectively, in BMDMs prior to thapsigargin treatment. Stimulation of any of these TLRs inhibited stress granule assembly, similar to TLR4 stimulation (Fig. 2A, 2B) suggesting that signaling downstream of either MyD88 or TRIF was sufficient to inhibit stress granule assembly. Stress granule inhibition was also independent of the subcellular localization of the TLR being stimulated. We further confirmed the importance of MyD88 and TRIF in mediating the TLR signaling to inhibit stress granule formation by testing the effect of TLR stimulation in *Myd88*$^{-/-}$ *Trif*$^{-/-}$ BMDMs. Stress granule inhibition was abrogated in the absence of MyD88 and TRIF (Fig. 2), providing additional evidence

that TLR signaling was responsible for stress granule assembly inhibition. To extend our findings and determine whether stress granules can be similarly inhibited in non-immune cells, we tested the effect of LPS, poly(I:C), and R848 stimulation on chemotherapy drug oxaliplatin mediated stress granule assembly in B16 melanoma cells. Stimulation with LPS, poly(I:C), and R848 inhibited oxaliplatin induced stress granule assembly, suggesting that innate signaling mediated inhibition occurs across cell types (Fig. 3). Taken together our results suggest that stress granule assembly can be inhibited by signaling downstream of MYD88 and TRIF in both immune and non-immune cells.

## TLR4 signaling can disassemble stress granules

Stress granules are dynamic membraneless compartments that can be disassembled when the stress is removed. The stress granule assembly – disassembly equilibrium has been reported to be controlled by post-translational modifications (12, 19). Similarly, the TLR signaling cascade involves a series of sequential post-translational modifications (13). Some of these post-translational modifications result in activation of transcription factors such as NF-κB that activate their target genes (13). A transcriptional response involves multiple steps – transcription, post-transcriptional processing of pre-mRNA, nuclear export, and translation, and stress granules inhibit translation of new proteins. While a transcriptional response takes time and would be impeded by stress granules, a signaling response based on post-translational modifications, such as phosphorylation, would be more rapid. Therefore, we used a time course analysis to monitor the kinetics of stress granule formation and to differentiate between the two types of responses. We first treated BMDMs with thapsigargin for 15, 30, 45, 60 and 90 minutes. Stress granules formed within 30 minutes of thapsigargin treatment (Fig. 4A, 4B). The number of stress granule-positive cells peaked after 60 minutes of thapsigargin treatment. Next, we tested the timing and duration of LPS stimulation required for stress granule inhibition. We stimulated BMDMs with LPS for 15 minutes,1 hour, or 4 hours prior to addition of thapsigargin, followed by incubation for 90 minutes. LPS stimulation for 15 minutes was sufficient to inhibit stress granule assembly (Fig. 5A). Additionally, the 15 minute LPS stimulation inhibited stress granules better than 1 hour and 4 hours of treatment. The rapid effect of LPS stimulation suggests that stress granule inhibition is primarily driven by a post-translational modification-based mechanism.

To test whether LPS stimulation can disassemble stress granules that are already formed, we performed a time course analysis in which we added LPS at different time points: together with or after 15, 30, 45 or 60 minutes of thapsigargin treatment. There was a decrease in the percentage of stress granule-positive cells at every time point of LPS addition, suggesting that LPS stimulation can disassemble the stress granules that are already formed (Fig. 5B, 5C). Since stress granule assembly leads to general translation arrest, disassembly is unlikely to be caused by TLR4-mediated transcriptional response which would require new protein synthesis to have an effect. Taken together, time course analysis suggests that stress granule inhibition is likely driven by post-translational modifications.

## LPS-induced MAP kinase activity is dispensable for stress granule inhibition

We next sought to identify the signaling pathway responsible for stress granule inhibition/ disassembly downstream of TLR4. Stress granule assembly could be affected by the

abundance of critical stress granule proteins G3BP1 and DDX3X, but we did not observe a decrease in the amounts of G3BP1 and DDX3X in response to LPS stimulation during thapsigargin treatment (Fig. 6A). We also did not observe a difference in eIF2α phosphorylation (Fig. 6A). We used western blot analysis to screen signaling pathways downstream of TLR4 for their role in stress granule inhibition/disassembly. LPS stimulation of TLR4 activates ERK1/2 and NF-κB signaling (13). To test the status of these signaling pathways during thapsigargin treatment, we performed western blot analysis of phospho- and total-ERK1/2 and phospho- and total-IκBα. We stimulated BMDMs for 1 hour with LPS followed by thapsigargin treatment for different durations. Over time, there was a decrease in basal ERK1/2 phosphorylation in BMDMs treated with thapsigargin alone. ERK1/2 phosphorylation remained elevated at every time point in BMDMs treated with thapsigargin and stimulated with LPS (Fig. 6A). We did not detect IκBα phosphorylation in BMDMs treated with thapsigargin alone. As expected, we observed increased phospho-IκBα in thapsigargin and LPS-treated BMDMs (Fig. 6A). Additionally, SAPKs, including P38 and JNK, are involved in both TLR and stress signaling (12, 13, 19). In BMDMs stimulated with thapsigargin alone, P38 phosphorylation increased within 15 minutes and then decreased over time (Fig. 6B). LPS stimulation alone induced P38 phosphorylation that was higher than that observed with thapsigargin treatment at any time point. In LPS and thapsigargin-stimulated BMDMs, P38 phosphorylation did not cycle and remained high regardless of the duration of thapsigargin treatment. In BMDMs stimulated with thapsigargin alone, JNK phosphorylation followed a similar trend as P38 phosphorylation (Fig. 6B). In LPS and thapsigargin-stimulated BMDMs, there was increased JNK phosphorylation at every time point compared to the corresponding time point in thapsigargin alone treatment. Since our time course experiment had suggested that stress granule inhibition and disassembly were driven by post-translational modifications (Fig. 4 and Fig. 5), we hypothesized that one of the three MAP kinases whose activity was modified by LPS stimulation would be required for the process. Therefore, we used small molecule inhibitors against these kinases and tested their effect on stress granule assembly in the presence or absence of LPS stimulation. To test the effect of P38 kinase activity inhibition, we stimulated BMDMs with 10 μM SB203580 with or without LPS treatment for 1 hour before adding thapsigargin. We observed that inhibition of P38 did not affect stress granule assembly in BMDMs (Supplemental Fig. 2A, 2B). To test the effect of JNK kinase activity inhibition, we stimulated BMDMs with 25 μM SP600125 with or without LPS treatment for 1 hour before adding thapsigargin and found that JNK kinase activity inhibition also did not affect stress granule assembly (Supplemental Fig. 3A, 3B). Finally, to test the effect of ERK1/2 kinase activity inhibition, we stimulated BMDMs with 10 μM U0126 with our without LPS for 1 hour. We found that ERK1/2 inhibition in the absence of LPS stimulation inhibited stress granule assembly and did not rescue it in LPS-stimulated BMDMs (Fig. 7A, 7B). Interpretation of the effect of LPS in this context is complicated by the observation that stress granule assembly was inhibited by U0126 treatment in the absence of LPS stimulation. Taken together our data suggest that LPS stimulation modifies MAP kinase activity in response to stress signaling. However, LPS-mediated inhibition of stress granule assembly is not dependent on P38, JNK, or ERK1/2 kinase activity.

### IKK inhibition rescues stress granule assembly in LPS stimulated BMDMs

To identify the signaling pathway responsible for stress granule inhibition or promotion of stress granule disassembly, we focused on kinases, since phosphorylation can modulate stress granule dynamics (12, 19). In addition to the MAP kinases, the IKK complex is also activated in response to TLR stimulation, and we had observed increased IκBα phosphorylation in LPS-treated BMDMs (Fig. 6A). Since the IKK complex has targets other than IκBα, we hypothesized that IKK activity might be responsible for the inhibition of stress assembly (20, 21). We treated BMDMs with 20 μM BMS345541 with or without LPS stimulation for 1 hour followed by thapsigargin treatment. BMS345541 treatment rescued stress granule assembly in LPS-stimulated BMDMs (Fig. 8A, 8B). To understand the mechanism of IKK mediated stress granule assembly inhibition, we performed western blot analysis of stress granule components DDX3X and G3BP1, and checked the status of signaling kinases upstream and downstream of the IKK complex. Since simultaneous addition of LPS with thapsigargin was sufficient to inhibit stress granule assembly in the time course analysis (Fig. 5B, 5C), we added LPS, thapsigargin, and/or BMS345541 simultaenously. IKK inhibition did not not increase the amounts of DDX3X and G3BP1, suggesting that stress granule assembly resuce was not due to increased expression of these proteins (Fig. 9A). IKK inhibition delayed IKKβ phosphorylation, and the amount of phosphorylated IKKβ (p-IKKβ) remained high in BMS345541-treated cells after 60 minutes of LPS stimulation (Fig. 9A). Phosphorylation of IKKβ in this context is most likely due to activity of IRAK1/4 kinases activated by myddosome assembly (17, 18). To determine whether IRAK1/4 had a role in stress granule inhibition, we tested the effect of IRAK1/4 kinase activity inhibition on stress granule assembly. IRAK1/4 inhibition did not rescue stress granule assembly, ruling out a role for these kinases in this process (Supplemental Fig. 4A, 4B). IKK kinase activity also leads to activation of NF-κB signaling through phosphorylation induced ubiquitination and proteosomal degradation of IκBα (17, 18). The NF-κB signaling pathway undergoes cyclical activation and inhibition, and is mirrored in IκBα phosphorylation and degradation kinetics (17, 18). As expected, BMS345541 treatment inhibited these cyclical IκBα dynamics (Fig. 9A). To test the effect of NF-κB inhibition on cytokine expression we performed qPCR analysis of *Il1b* and *Ifnb* in BMDMs stimulated with LPS for 1 hour followed by thapsigargin stimulation for another hour. Expression of *Il1b* was severely diminished in BMS345541 treated BMDMs (Fig. 9B). Expression of *Ifnb,* which does not strictly depend on NF-κB signaling (17), was not reduced by BMS345541 treatment (Fig. 9C). Additionally, translation initiation regulator eIF2α phosphorylation can trigger stress granule assembly (3). However, BMS345541 treatment did not increase the amounts of phosphorylated eIF2α (p-eIF2α) (Fig. 9A). BMS345541 treatment also did not affect the amounts of phosphorylated RPS6 and AKT, suggesting that stress granule inhibition was not mediated by increased mTOR activity (Fig. 9A) (17). Taken together, our data suggest that stress granule inhibition by TLR signaling is mediated by IKK kinase activity and is independent of eIF2α phosphorylation, mTOR activity, and abundances of DDX3X and G3BP1.

## DISCUSSION

Stress granules are dynamic membraneless compartments that allow cells to survive a stressed condition. Defects in stress granule dynamics or stress granule components have been implicated in human diseases including cancers and neurodegenerative diseases (22–26). The molecular mechanism controlling stress granule assembly and disassembly is not well understood. We discovered that TLR stimulation can lead to a defect in stress granule assembly induced by ER stress. The rapid effect of TLR4 signaling in time course kinetics analysis suggested that this inhibition was likely driven by post-translational modifications.

We screened for kinases that might be involved in regulating stress granule dynamics using chemical inhibitors of SAPK-mediated phosphorylation that have previously been reported to modulate stress granule dynamics (12, 19). However, SAPK inhibition failed to rescue stress granule assembly. Our data suggest that the IKK complex plays a central role in inhibition of stress granule assembly and disassembly of stress granules formed prior to PRR stimulation. The target of the IKK complex responsible for stress granule inhibition and disassembly remains unclear. It is likely that IKK-mediated phosphorylation of a critical stress granule component is changing its liquid-liquid phase separation (LLPS) behavior (16, 25, 27, 28). The IKK complex can be activated downstream of endogenous DAMPs and pro-inflammatory cytokines IL-1α and IL-1β (29). This suggests that persistent sterile inflammation can interfere with stress granule-mediated inhibition of programmed cell death. Since aberrant programmed death leads to the release of DAMPs, along with IL-1α and IL-1β, this can create a self-reinforcing feedback loop that worsens an inflammatory condition (30–34).

Additionally, we had previously discovered that stress granules inhibit pyroptosis – a pro-inflammatory form of programmed cell death (4). Stress granules have also been reported to inhibit apoptosis (12). Innate immune signaling-mediated inhibition of stress granules could be enabling programmed cell death activation and making it inflammatory by promoting expression of pro-inflammatory cytokines for an optimal host response to pathogenic challenges (35–38). Furthermore, prion-like phase transitions associated with NLRP3 inflammasome activation have been implicated in neurodegenerative diseases (39). This suggests that inhibition of stress granule assembly or disassembly of existing stress granules can promote prionoid phase transition over LLPS that might promote neurodegeneration. Stress granules have also been reported to promote resistance to cancer chemotherapy (26, 40). Our observation here that oxaliplatin induced stress granules are inhibited by innate immune signaling suggests that addition of TLR agonists to treatment regimens with stress granule inducing chemotherapeutics may improve efficacy. Taken together, we have discovered a novel link between stress and innate immune response signaling pathways. The crosstalk between innate immune signaling and stress granules can be an important target for therapeutic interventions in human diseases.

## Supplementary Material

Refer to Web version on PubMed Central for supplementary material.

## ACKNOWLEDGEMENTS

We thank all the members of the Kanneganti laboratory for their suggestions. We thank Rebecca Tweedell, PhD, for scientific editing of the manuscript.

This study was supported by grants from the US National Institutes of Health (AR056296, CA253095, AI101935 and AI124346) and the American Lebanese Syrian Associated Charities to T.D.-K. The content is solely the responsibility of the authors and does not necessarily represent the official views of the National Institutes of Health.

## REFERENCES

1. Corbet GA, and Parker R. 2020. RNP Granule Formation: Lessons from P-Bodies and Stress Granules. Cold Spring Harbor Symposia on Quantitative Biology: 040329.
2. Kedersha NL, Gupta M, Li W, Miller I, and Anderson P. 1999. RNA-Binding Proteins Tia-1 and Tiar Link the Phosphorylation of Eif-2α to the Assembly of Mammalian Stress Granules. The Journal of Cell Biology 147: 1431–1442. [PubMed: 10613902]
3. Protter DSW, and Parker R. 2016. Principles and Properties of Stress Granules. Trends in Cell Biology 26: 668–679. [PubMed: 27289443]
4. Samir P, Kesavardhana S, Patmore DM, Gingras S, Malireddi RKS, Karki R, Guy CS, Briard B, Place DE, Bhattacharya A, Sharma BR, Nourse A, King SV, Pitre A, Burton AR, Pelletier S, Gilbertson RJ, and Kanneganti T-D. 2019. DDX3X acts as a live-or-die checkpoint in stressed cells by regulating NLRP3 inflammasome. Nature 573: 590–594. [PubMed: 31511697]
5. Khaperskyy DA, Hatchette TF, and McCormick C. 2012. Influenza A virus inhibits cytoplasmic stress granule formation. FASEB J 26: 1629–1639. [PubMed: 22202676]
6. Onomoto K, Yoneyama M, Fung G, Kato H, and Fujita T. 2014. Antiviral innate immunity and stress granule responses. Trends in Immunology 35: 420–428. [PubMed: 25153707]
7. Poblete-Durán N, Prades-Pérez Y, Vera-Otarola J, Soto-Rifo R, and Valiente-Echeverría F. 2016. Who Regulates Whom? An Overview of RNA Granules and Viral Infections. Viruses 8: 180. [PubMed: 27367717]
8. Thulasi Raman SN, Liu G, Pyo HM, Cui YC, Xu F, Ayalew LE, Tikoo SK, and Zhou Y. 2016. DDX3 Interacts with Influenza A Virus NS1 and NP Proteins and Exerts Antiviral Function through Regulation of Stress Granule Formation. Journal of Virology 90: 3661–3675. [PubMed: 26792746]
9. Tsai WC, and Lloyd RE. 2014. Cytoplasmic RNA Granules and Viral Infection. Annu Rev Virol 1: 147–170. [PubMed: 26958719]
10. White JP, and Lloyd RE. 2012. Regulation of stress granules in virus systems. Trends in Microbiology 20: 175–183. [PubMed: 22405519]
11. Kesavardhana S, Samir P, Zheng M, Malireddi RKS, Karki R, Sharma BR, Place DE, Briard B, Vogel P, and Kanneganti T-D. DDX3X coordinates host defense against influenza virus by activating the NLRP3 inflammasome and type I interferon response. Journal of Biological Chemistry.
12. Arimoto K, Fukuda H, Imajoh-Ohmi S, Saito H, and Takekawa M. 2008. Formation of stress granules inhibits apoptosis by suppressing stress-responsive MAPK pathways. Nature Cell Biology 10: 1324–1332. [PubMed: 18836437]
13. Oda K, and Kitano H. 2006. A comprehensive map of the toll-like receptor signaling network. Molecular Systems Biology 2: 2006.0015.
14. Briard B, Karki R, Malireddi RKS, Bhattacharya A, Place DE, Mavuluri J, Peters JL, Vogel P, Yamamoto M, and Kanneganti T-D. 2019. Fungal ligands released by innate immune effectors promote inflammasome activation during Aspergillus fumigatus infection. Nature Microbiology 4: 316–327.
15. Karki R, Lee E, Place D, Samir P, Mavuluri J, Sharma BR, Balakrishnan A, Malireddi RKS, Geiger R, Zhu Q, Neale G, and Kanneganti T-D. 2018. IRF8 Regulates Transcription of Naips for NLRC4 Inflammasome Activation. Cell 0.
16. Wheeler JR, Matheny T, Jain S, Abrisch R, and Parker R. 2016. Distinct stages in stress granule assembly and disassembly. eLife 5: e18413. [PubMed: 27602576]

17. Fitzgerald KA, and Kagan JC. 2020. Toll-like Receptors and the Control of Immunity. Cell 180: 1044–1066. [PubMed: 32164908]
18. Kawai T, and Akira S. 2007. TLR signaling. Seminars in Immunology 19: 24–32. [PubMed: 17275323]
19. Aditi A, Mason AC, Sharma M, Dawson TR, and Wente SR. 2018. MAPK- and glycogen synthase kinase 3–mediated phosphorylation regulates the DEAD-box protein modulator Gle1 for control of stress granule dynamics. Journal of Biological Chemistry: jbc.RA118.005749.
20. Huang W-C, and Hung M-C. 2013. Beyond NF-κB activation: nuclear functions of IκB kinase α. Journal of Biomedical Science 20: 3. [PubMed: 23343355]
21. Liu F, Xia Y, Parker AS, and Verma IM. 2012. IKK biology. Immunological Reviews 246: 239–253. [PubMed: 22435559]
22. Boeynaems S, Bogaert E, Kovacs D, Konijnenberg A, Timmerman E, Volkov A, Guharoy M, De Decker M, Jaspers T, Ryan VH, Janke AM, Baatsen P, Vercruysse T, Kolaitis R-M, Daelemans D, Taylor JP, Kedersha N, Anderson P, Impens F, Sobott F, Schymkowitz J, Rousseau F, Fawzi NL, Robberecht W, Van Damme P, Tompa P, and Van Den Bosch L. 2017. Phase Separation of C9orf72 Dipeptide Repeats Perturbs Stress Granule Dynamics. Molecular Cell 65: 1044–1055.e1045. [PubMed: 28306503]
23. Valentin-Vega YA, Wang Y-D, Parker M, Patmore DM, Kanagaraj A, Moore J, Rusch M, Finkelstein D, Ellison DW, Gilbertson RJ, Zhang J, Kim HJ, and Taylor JP. 2016. Cancer-associated DDX3X mutations drive stress granule assembly and impair global translation. Scientific Reports 6: 25996. [PubMed: 27180681]
24. Wolozin B 2012. Regulated protein aggregation: stress granules and neurodegeneration. Molecular Neurodegeneration 7: 56. [PubMed: 23164372]
25. Yang P, Mathieu C, Kolaitis R-M, Zhang P, Messing J, Yurtsever U, Yang Z, Wu J, Li Y, Pan Q, Yu J, Martin EW, Mittag T, Kim HJ, and Taylor JP. 2020. G3BP1 Is a Tunable Switch that Triggers Phase Separation to Assemble Stress Granules. Cell 181: 325–345.e328. [PubMed: 32302571]
26. Grabocka E, and Bar-Sagi D. 2016. Mutant KRAS Enhances Tumor Cell Fitness by Upregulating Stress Granules. Cell 167: 1803–1813.e1812. [PubMed: 27984728]
27. Mittag T, and Parker R. 2018. Multiple Modes of Protein–Protein Interactions Promote RNP Granule Assembly. Journal of Molecular Biology.
28. Samir P, and Kanneganti T-D. 2020. DDX3X Sits at the Crossroads of Liquid–Liquid and Prionoid Phase Transitions Arbitrating Life and Death Cell Fate Decisions in Stressed Cells. DNA and Cell Biology 39: 1091–1095. [PubMed: 32397752]
29. Lukens J, Gross J, and Kanneganti T-D. 2012. IL-1 family cytokines trigger sterile inflammatory disease. Frontiers in Immunology 3.
30. Malireddi RKS, Gurung P, Kesavardhana S, Samir P, Burton A, Mummareddy H, Vogel P, Pelletier S, Burgula S, and Kanneganti T-D. 2019. Innate immune priming in the absence of TAK1 drives RIPK1 kinase activity–independent pyroptosis, apoptosis, necroptosis, and inflammatory diseaseRIPK1 kinase activity–independent cell death and inflammasome activation. Journal of Experimental Medicine 217.
31. Ruera CN, Miculán E, Pérez F, Ducca G, Carasi P, and Chirdo FG. 2021. Sterile inflammation drives multiple programmed cell death pathways in the gut. Journal of Leukocyte Biology 109: 211–221. [PubMed: 32946645]
32. Bedoui S, Herold MJ, and Strasser A. 2020. Emerging connectivity of programmed cell death pathways and its physiological implications. Nature Reviews Molecular Cell Biology 21: 678–695. [PubMed: 32873928]
33. Samir P, Malireddi RKS, and Kanneganti T-D. 2020. The PANoptosome: A Deadly Protein Complex Driving Pyroptosis, Apoptosis, and Necroptosis (PANoptosis). Frontiers in Cellular and Infection Microbiology 10.
34. Christgen S, Zheng M, Kesavardhana S, Karki R, Malireddi RKS, Banoth B, Place DE, Briard B, Sharma BR, Tuladhar S, Samir P, Burton A, and Kanneganti T-D. 2020. Identification of the PANoptosome: A Molecular Platform Triggering Pyroptosis, Apoptosis, and Necroptosis (PANoptosis). Frontiers in Cellular and Infection Microbiology 10.

35. Bauernfeind FG, Horvath G, Stutz A, Alnemri ES, MacDonald K, Speert D, Fernandes-Alnemri T, Wu J, Monks BG, Fitzgerald KA, Hornung V, and Latz E. 2009. Cutting Edge: NF-κB Activating Pattern Recognition and Cytokine Receptors License NLRP3 Inflammasome Activation by Regulating NLRP3 Expression. The Journal of Immunology 183: 787–791. [PubMed: 19570822]

36. Gaidt MM, and Hornung V. 2018. The NLRP3 Inflammasome Renders Cell Death Pro-inflammatory. Journal of Molecular Biology 430: 133–141. [PubMed: 29203171]

37. Kanneganti T-D, Body-Malapel M, Amer A, Park J-H, Whitfield J, Franchi L, Taraporewala ZF, Miller D, Patton JT, Inohara N, and Núñez G. 2006. Critical Role for Cryopyrin/Nalp3 in Activation of Caspase-1 in Response to Viral Infection and Double-stranded RNA. Journal of Biological Chemistry 281: 36560–36568. [PubMed: 17008311]

38. Thomas PG, Dash P, Aldridge JR, Ellebedy AH, Reynolds C, Funk AJ, Martin WJ, Lamkanfi M, Webby RJ, Boyd KL, Doherty PC, and Kanneganti T-D. 2009. The Intracellular Sensor NLRP3 Mediates Key Innate and Healing Responses to Influenza A Virus via the Regulation of Caspase-1. Immunity 30: 566–575. [PubMed: 19362023]

39. Heneka MT, Kummer MP, Stutz A, Delekate A, Schwartz S, Vieira-Saecker A, Griep A, Axt D, Remus A, Tzeng T-C, Gelpi E, Halle A, Korte M, Latz E, and Golenbock DT. 2013. NLRP3 is activated in Alzheimer's disease and contributes to pathology in APP/PS1 mice. Nature 493: 674–678. [PubMed: 23254930]

40. Adjibade P, Simoneau B, Ledoux N, Gauthier W-N, Nkurunziza M, Khandjian EW, and Mazroui R. 2020. Treatment of cancer cells with Lapatinib negatively regulates general translation and induces stress granules formation. PLOS ONE 15: e0231894. [PubMed: 32365111]

## KEY POINTS

1. Innate immune signaling through TLRs affects stress granule assembly.
2. TLR signaling promotes disassembly of stress granules that are already formed.
3. Stress granule inhibition is dependent on the kinase activity of the IKK complex.

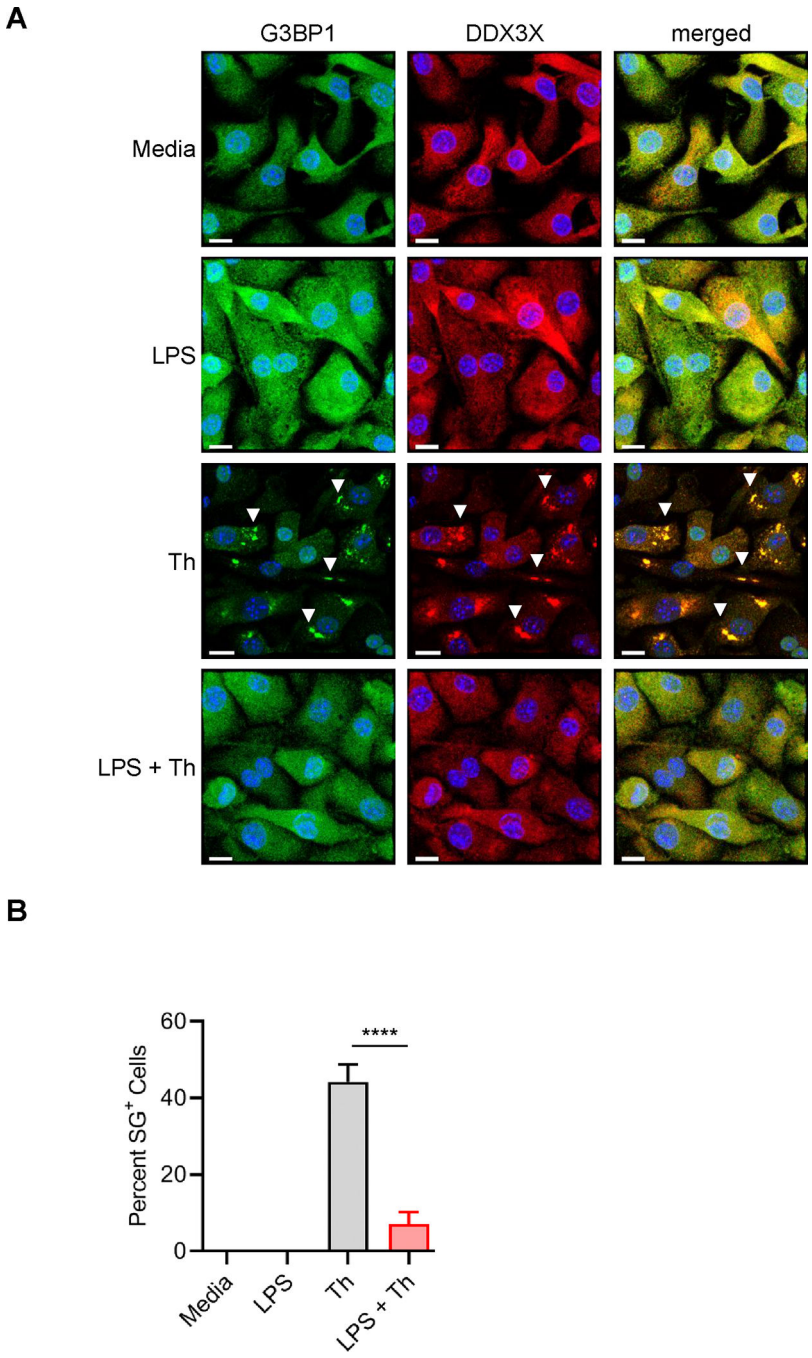


**Figure 1: LPS induced signaling inhibits thapsigargin mediated stress granule assembly.**

(A) Confocal microscopy images of BMDMs stimulated with 100 ng/mL LPS for 4 hours, 2 μg/mL thapsigargin (Th) for 90 minutes, or 100 ng/mL LPS for 4 hours followed by 2 μg/mL thapsigargin treatment for 90 minutes (LPS + Th). Scale bar represents 10 μm. (B) Quantification of percentage of stress granule positive cells. One-way ANOVA was used for statistical analysis. **** represents p-value < 0.0001. Representative images and quantification are shown that were generated from one of the replicates (n > 3).

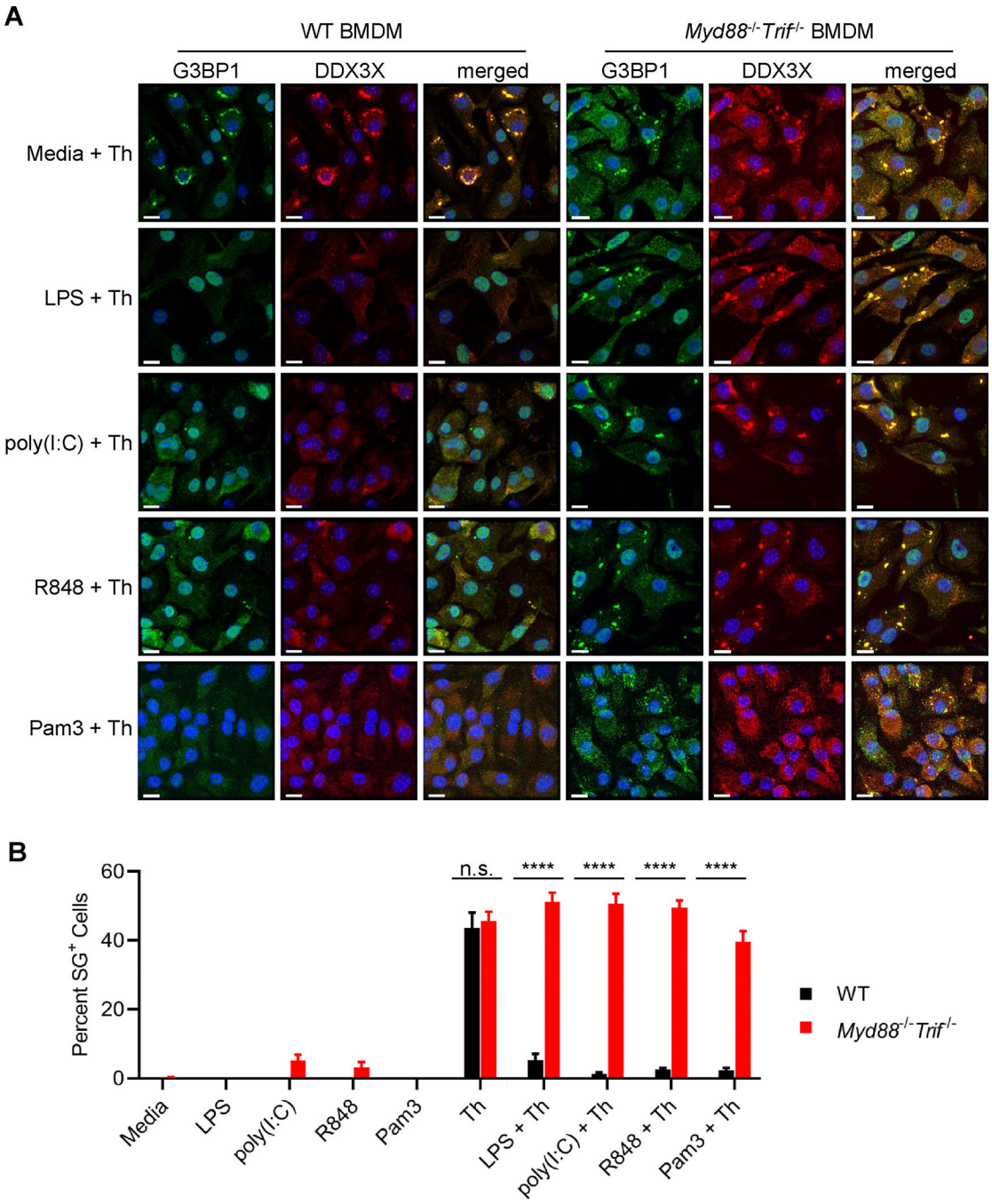


**Figure 2: Signaling downstream of MYD88 and TRIF inhibits thapsigargin mediated stress granule assembly.**

(A) Confocal microscopy images of WT and *Myd88*$^{-/-}$ *Trif*$^{-/-}$ BMDMs stimulated with 2 μg/mL thapsigargin (Th) for 90 minutes, 100 ng/mL LPS for 4 hours followed by 2 μg/mL thapsigargin for 90 minutes (LPS + Th), 50 μg/mL poly(I:C) for 4 hours followed by 2 μg/mL thapsigargin for 90 minutes (poly(I:C) + Th), 1 μg/mL R848 for 4 hours followed by 2 μg/mL thapsigargin for 90 minutes (R848 + Th), or 1 μg/mL Pam3CSK4 for 4 hours followed by 2 μg/mL thapsigargin for 90 minutes (Pam3 + Th). Scale bar represents 10 μm. (B) Quantification of percentage of stress granule positive cells. Two-way ANOVA was used

for statistical analysis. **** represents p-value < 0.0001, n.s. represents lack of statistical significance at alpha level of 0.05. Representative images and quantification are shown that were generated from one of the replicates (n = 3).

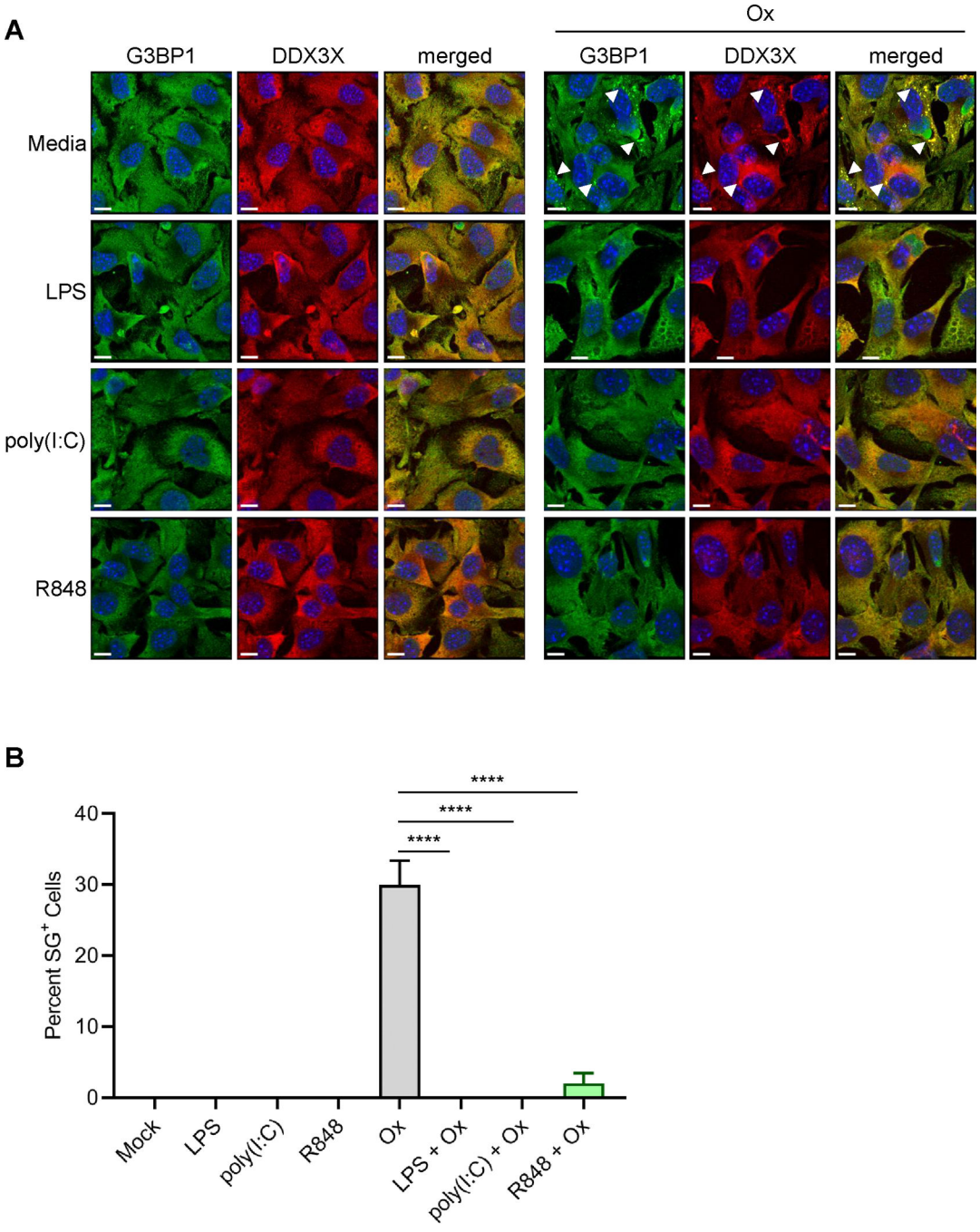


**Figure 3: : Innate immune signaling inhibits oxaliplatin mediated stress granule assembly in B16 melanoma cells.**

(A) Confocal microscopy images of B16 melanoma cell treated with 100 μM oxaliplatin (Ox) for 4 hours with or without prior stimulation for 4 hours with 100 ng/mL LPS, 50 μg/mL poly(I:C), or 2 μg/mL R848. Scale bar represents 10 μm. (B) Quantification of percentage of stress granule positive cells. One-way ANOVA was used for statistical analysis. **** represents p-value < 0.0001. Representative images and quantification are shown that were generated from one of the replicates (n = 3).

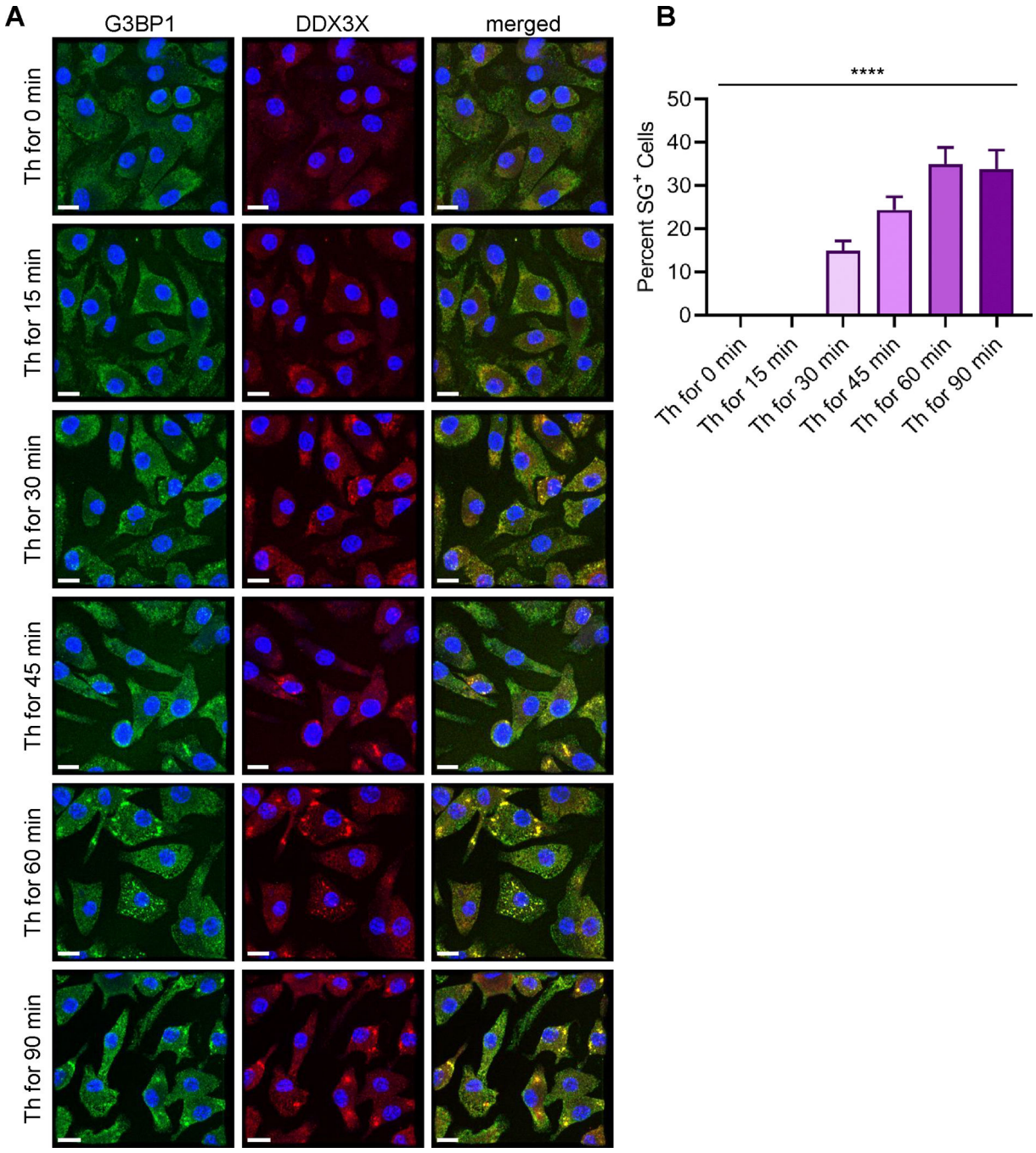


**Figure 4: Stress granules begin to appear within 30 minutes of thapsigargin treatment.**

(A) Confocal microscopy images of BMDMs treated with 2 μg/mL thapsigargin (Th) for 0, 15, 30, 45, 60, or 90 minutes. Scale bar represents 10 μm. (B) Quantification of percentage of stress granule positive cells. One-way ANOVA was used for statistical analysis. Reported p-value is for the effect of duration of thapsigargin treatment. **** represents p-value < 0.0001. Representative images (n = 3). Graph was generated from pooled data from the three replicates.

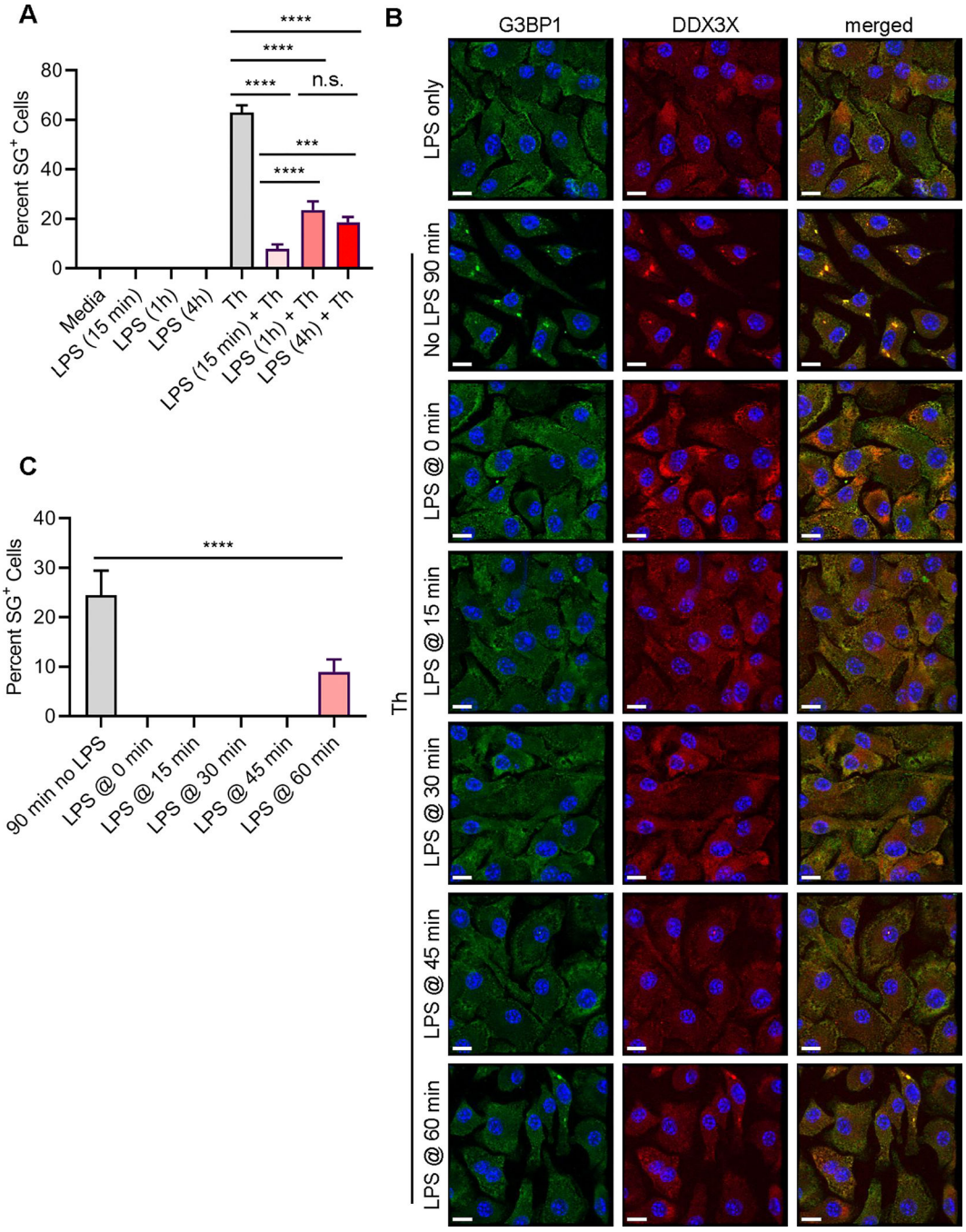


**Figure 5: LPS stimulation promotes disassembly of stress granules.**

(A) Quantification of the effect of different durations of LPS stimulation on stress granule inhibition. BMDMs were stimulated with 100 ng/mL LPS for 15 minutes, 1 hour, or 4 hours before treatment with 2 μg/mL thapsigargin for 90 minutes (Th). (B) Confocal microscopy images of BMDMs treated with 2 μg/mL thapsigargin for 90 minutes. 100 ng/mL LPS was added either together with thapsigargin (LPS @ 0 min) or at 15 (LPS @ 15 min), 30 (LPS @ 30 min), 45 (LPS @ 45 min), or 60 (LPS @ 60 min) minutes after thapsigargin. Scale bar represents 10 μm. (C) Quantification of percentage of stress granule positive cells. One-way

ANOVA was used for statistical analysis. **** represents p-value < 0.0001, n.s. represents lack of statistical significance at alpha level of 0.05. Representative images (n = 2). Graph was generated from pooled data from the two replicates.

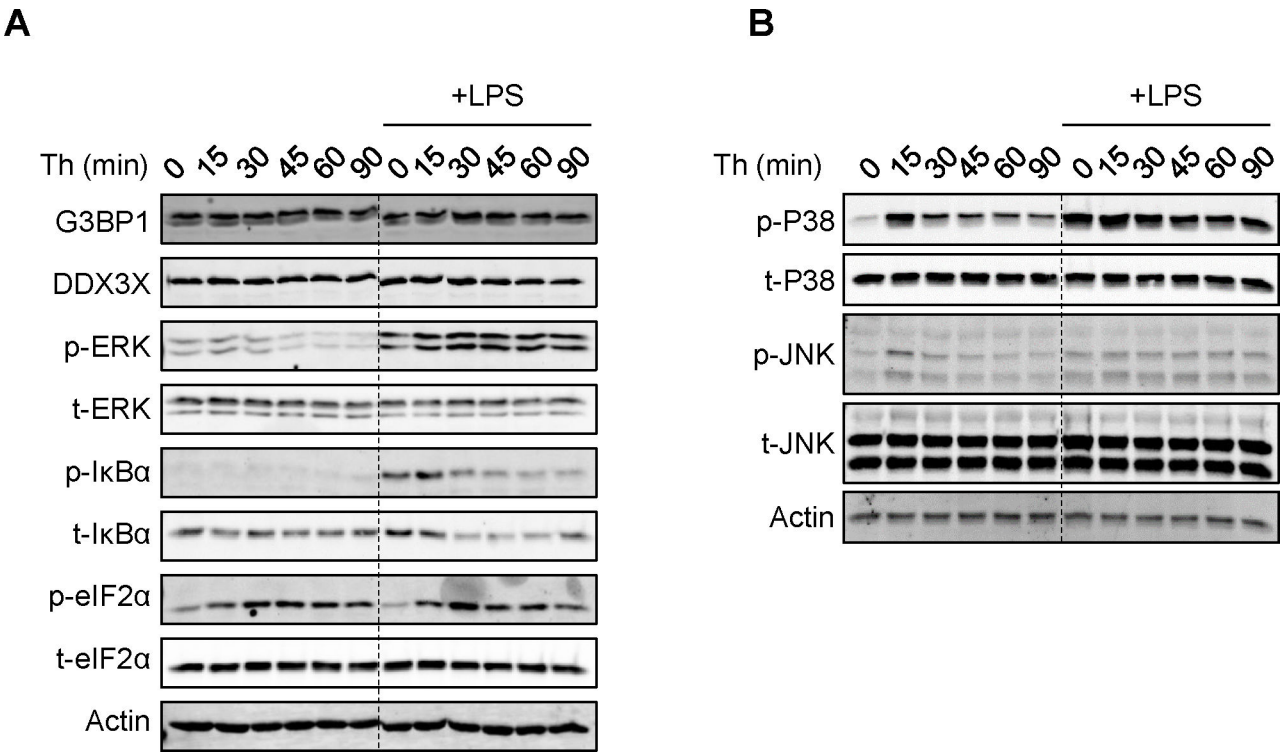


**Figure 6: Thapsigargin treatment modifies ERK1/2, P38 and JNK activation.**

(A) Western blot analysis of G3BP1, DDX3X, phosphorylated ERK1/2 (p-ERK), total-ERK1/2 (t-ERK), phosphorylated IκBα (p-IκBα), total IκBα (t-IκBα), phosphorylated eIF2α (p- eIF2α), total eIF2α (t- eIF2α), and actin in BMDMs treated with thapsigargin (Th) alone for the indicated durations or stimulated with LPS for 1 hour followed by thapsigargin treatment for the indicated time. (B) Western blot analysis of phosphorylated P38 (p-P38), total P38 (t-P38), phosphorylated JNK (p-JNK), total JNK (t-JNK), and actin in BMDMs treated with thapsigargin (Th) alone for the indicated durations or stimulated with LPS for 1 hour followed by thapsigargin treatment for the indicated time. Representative blots (n = 3).

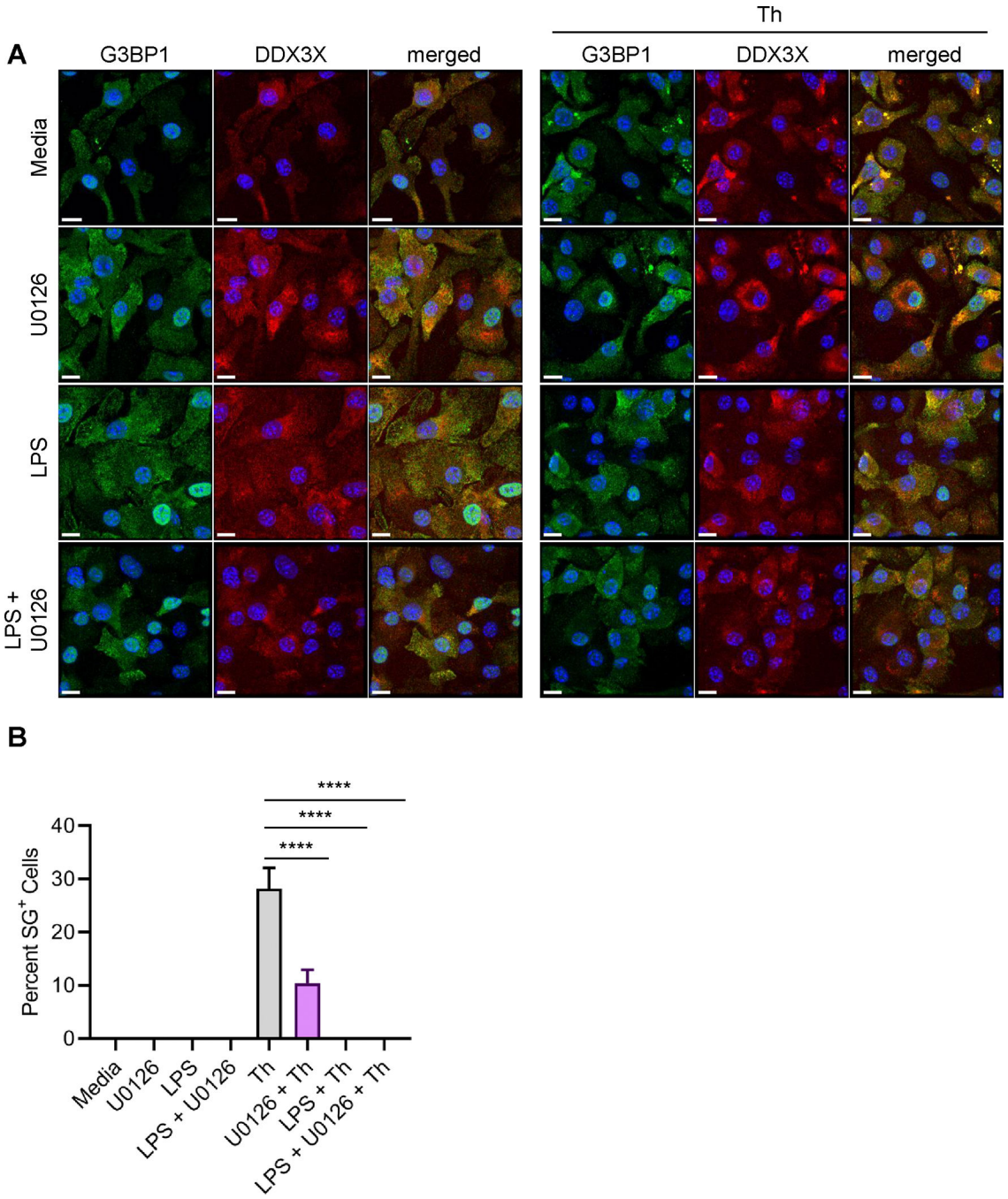


**Figure 7: Inhibition of ERK1/2 kinase activity represses stress granule assembly.**

(A) Confocal microscopy images of BMDMs treated with 2 μg/mL thapsigargin (Th) for 90 minutes in the presence or absence of 10 μM ERK1/2 inhibitor U0126 with or without LPS stimulation for 1 hour. U0126 was added at the same time with LPS. Scale bar represents 10 μm. (B) Quantification of percentage of stress granule positive cells. One-way ANOVA was used for statistical analysis. **** represents p-value < 0.0001. Representative images and quantification are shown that were generated from one of the replicates (n = 3).

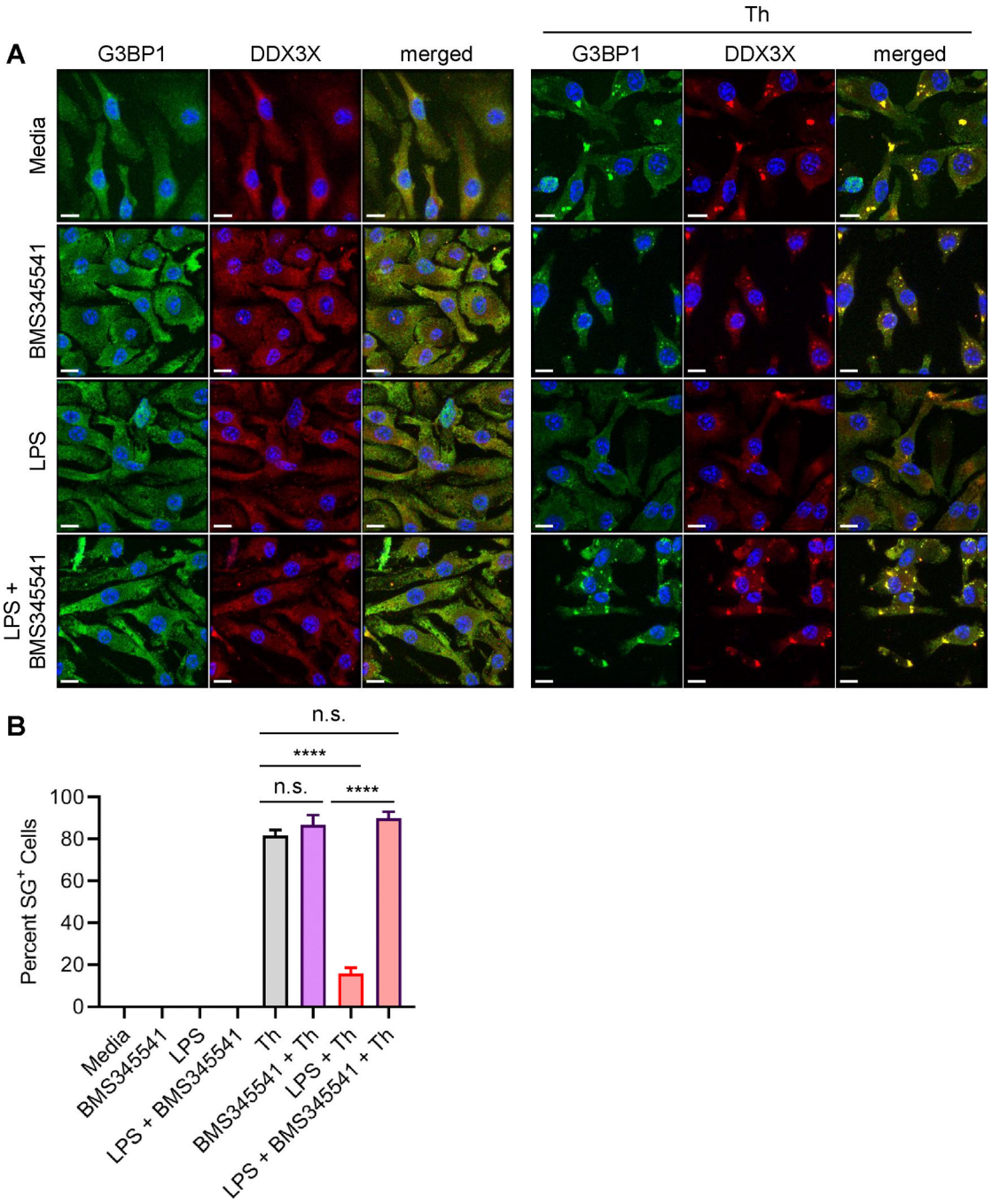


**Figure 8: Inhibition of IKK complex kinase activity rescues stress granule assembly.**

(A) Confocal microscopy images of BMDMs treated with 2 μg/mL thapsigargin (Th) for 90 minutes in the presence or absence of 20 μM IKK complex inhibitor BMS345541 with or without LPS stimulation for 1 hour. BMS345541 was added at the same time with LPS. Scale bar represents 10 μm. (B) Quantification of percentage of stress granule positive cells. One-way ANOVA was used for statistical analysis. **** represents p-value < 0.0001, n.s. represents lack of statistical significance at alpha level of 0.05. Representative images and quantification are shown that were generated from one of the replicates (n = 3).

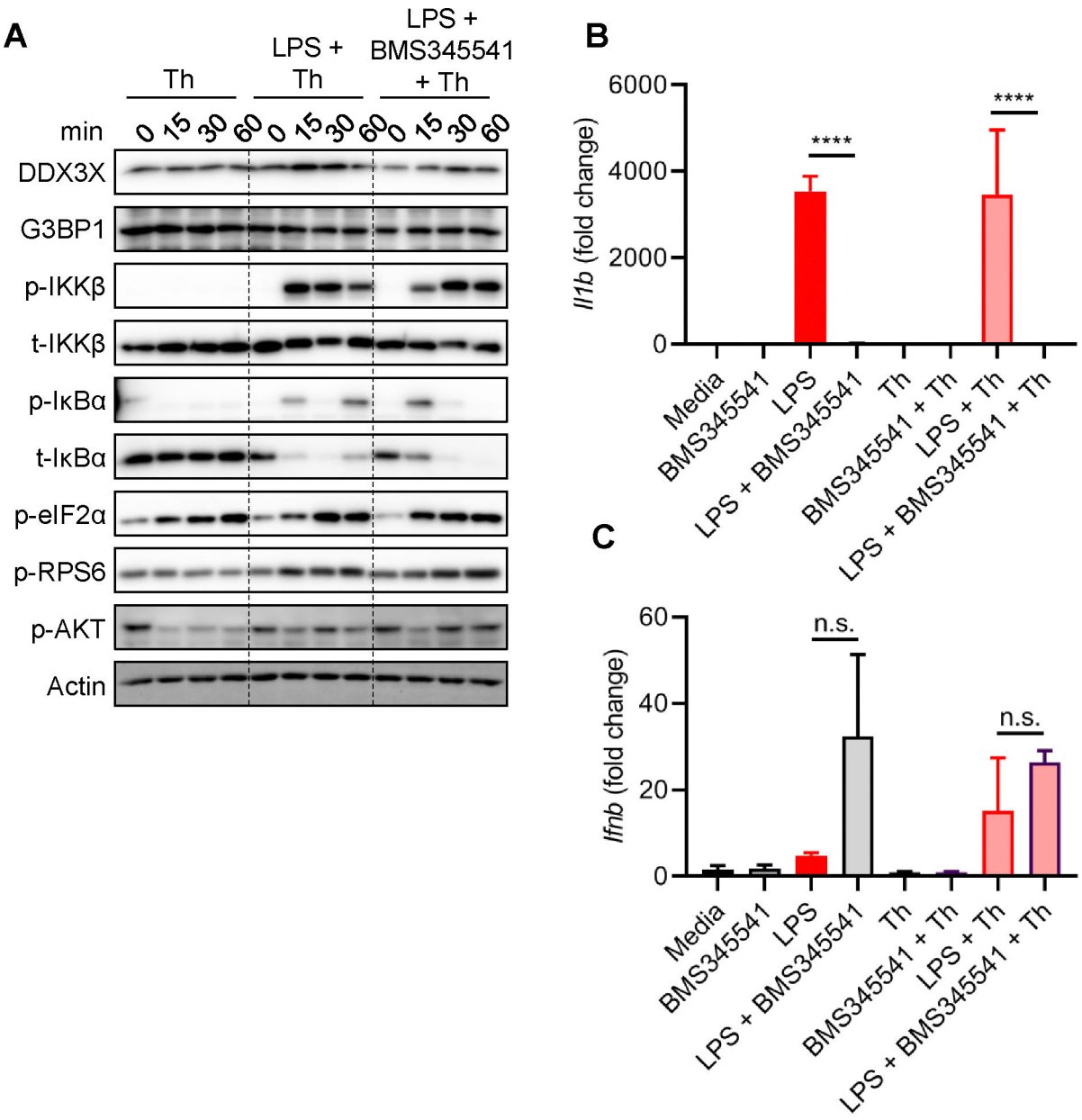


**Figure 9: IKK complex mediated inhibition of stress granule assembly is independent of the amounts of DDX3X and G3BP1, and mTOR signaling.**

(A) Western blot analysis of DDX3X, G3BP1, phosphorylated and total IKKβ (p-IKKβ and t-IKKβ), phosphorylated and total IκBα (p-IκBα and t-IκBα), phosphorylated eIF2α (p-eIF2α), phosphorylated RPS6 (p-RPS6), phosphorylated AKT (p-AKT), and actin in BMDMs treated with 2 μg/mL thapsigargin (Th) with or without 100 ng/mL LPS in the presence or absence of 20 μM BMS345541. LPS, BMS345541, and thapsigargin were added simultaneously to the BMDMs. (B-C) Quantitative RT-PCR analysis of *Il1b* (B) and *Ifnb* (C) expression in BMDMs treated with 2 μg/mL thapsigargin (Th) with or without 100 ng/mL LPS in the presence or absence of 20 μM BMS345541. BMDMs were stimulated with LPS and/or BMS345541 for 1 hour followed by thapsigargin treatment for 1 hour. One-way ANOVA was used for statistical analysis. **** represents p-value < 0.0001, n.s. represents

lack of statistical significance at alpha level of 0.05. Representative graphs are shown and were generated from one of the replicates (n = 3).